

## Measurements of the Parallel and Perpendicular Ion Temperatures by Means of an Ion-sensitive Segmented Tunnel Probe

P. Balan<sup>1</sup>, R. Schrittwieser\*<sup>1</sup>, J. Adámek<sup>2</sup>, O. Bařina<sup>3</sup>, P. De Beule<sup>4</sup>, I. Ďuran<sup>2</sup>, J.P. Gunn<sup>5</sup>, R. Hrach<sup>2</sup>, M. Hron<sup>2</sup>, C. Ioniřa<sup>1</sup>, E. Martines<sup>6</sup>, R. Pánek<sup>2</sup>, J. Stöckel<sup>2</sup>, G. Van Den Berge<sup>4</sup>, G. Van Oost<sup>4</sup>, T. Van Rompuy<sup>4</sup>, and M. Vicher<sup>3</sup>

<sup>1</sup> Institute for Ion Physics, University of Innsbruck, Austria

<sup>2</sup> Institute of Plasma Physics, Association EURATOM-IPP.CR, Prague, Czech Republic

<sup>3</sup> Charles University in Prague, Faculty of Mathematics and Physics, Czech Republic

<sup>4</sup> Department of Applied Physics, Ghent University, Belgium

<sup>5</sup> Association EURATOM-CEA sur la fusion contrôlée, Saint Paul Lez Durance, France

<sup>6</sup> Consorzio RFX, Associazione EURATOM-ENEA sulla Fusione, Padova, Italy

Received 15 April 2004, accepted 15 April 2004

Published online 29 October 2004

**Key words** Fusion plasma, probe diagnostic, perpendicular ion temperature, parallel ion temperature.

**PACS** 52.25.Xz, 52.55.Fa, 52.65.Rr, 52.70.Nc,

Localised ion temperature measurements can only be performed with special electric probes where the electron component of the current is kept off from the collector. In a strong magnetic field the effect can be utilised that the electron gyro-radius is much smaller than that of the ions. This method was developed by Katsumata and Okazaki (Japan J. Appl. Phys. **6**, 123 (1967)). We have used a so-called tunnel probe (which consists of a conductive tunnel, terminated by an isolated back plate) by adding a diaphragm in front. Thereby the tunnel is prevented from incident electrons at any potential of both electrodes. By sweeping the potential across the tunnel, the perpendicular ion temperature can be inferred. By segmenting the tunnel axially in two parts also the parallel ion temperature can be determined. When the electrodes are biased to ion saturation, the ratio between the ion currents, which reach the first and the second segment, respectively, is a measure for the parallel ion temperature. The dependence of the ratio of the currents has to be determined by a PIC simulation.

© 2004 WILEY-VCH Verlag GmbH & Co. KGaA, Weinheim

### 1 Introduction

Measurements of the ion temperature  $T_i$  in a tokamak edge plasma are a difficult task. In order to determine the ion energy distribution with a probe it is necessary to remove the electron component of the incident plasma flux, since the exponential drop of the ion current, which delivers the ion temperature, is buried in the electron retarding field region. This imperative inspired the concept of the Katsumata ion-sensitive probe [1,2]. However, a reliable calibration of the Katsumata probe requires 3D, self-consistent particle-in-cell (PIC) simulations because the magnetic field is perpendicular to the cylindrical axis of the probe, which makes the ion trajectories very complicated and can give rise to an electron current to the collector due to an  $\mathbf{E} \times \mathbf{B}$  drift.

Recently a new kind of plasma probe was developed [3,4]. It was called “tunnel probe” with the main purpose of measuring the electron temperature  $T_e$ . In this case the magnetic field and cylindrical axis are parallel to each other. In this contribution we show how a slight modification of this probe transforms it into a kind of Katsumata probe, thereby providing access to measurements of the perpendicular ion temperature  $T_{i,\perp}$ . The addition of a small diaphragm in front of the orifice shields the concave tunnel surface from electrons. A retarding voltage is applied to the tunnel in order to scan the perpendicular ion energy distribution from which  $T_{i,\perp}$  can be determined.

When the tunnel is segmented axially into two parts, the ratio between the ion saturation current  $I_{i,2}$  to the second segment and  $I_{i,1}$  to the first one contains an information on the parallel ion energy distribution function so that it is possible to obtain a measure for the parallel ion temperature  $T_{i,\parallel}$  from this ratio. The rationale is that

\* Corresponding author: e-mail: Roman.Schrittwieser@uibk.ac.at, Phone: +43 512 507 6244, Fax: +43 512 507 2932

© 2004 WILEY-VCH Verlag GmbH & Co. KGaA, Weinheim

ions with a high parallel velocity component can make it to the second segment, whereas those ions with a small parallel velocity (having on the other hand a large perpendicular velocity component) will mainly be attracted by the first segment.

This probe geometry presents the advantage that it can be simulated easily using the XOOPIC code [5]. We report on the first measurements using such a configuration in the CASTOR tokamak and compare them with kinetic simulations of the ion current characteristic.

## 2 Experimental set-up method

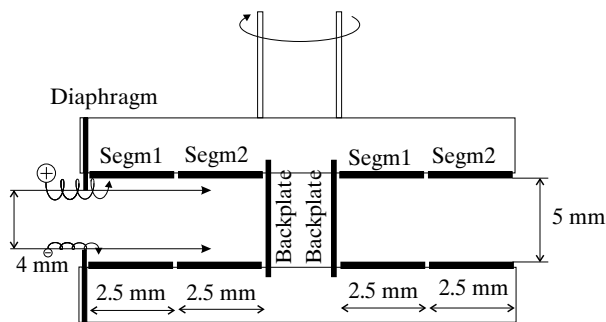


**Fig. 1** The ion-sensitive segmented Katsumata tunnel probe: the left-hand side shows the modified tunnel probe with a diaphragm in front, by which it becomes an ion-sensitive probe (Katsumata probe). The right-hand side probe is a purely segmented tunnel probe.

Fig. 1 shows the modified tunnel probe of which we have used only the left-hand part in this experiment. In front of the entrance orifice of the tunnel an additional diaphragm is mounted, which transforms it into an ion-sensitive (Katsumata) probe [1, 2, 6]. The tunnel has an inner diameter of 5 mm; the diaphragm an inner diameter of 4 mm. In addition, the tunnel electrode is segmented axially into two equally long parts of 2.5 mm length. All three electrodes are isolated from each other. The probe head is mounted on a manipulator allowing to move it radially on a shot to shot basis. Furthermore, it is possible to rotate the probe head to align its axis with the magnetic field lines and to orient the probe either upstream or downstream with respect to the direction of the toroidal plasma current.

All electrodes (diaphragm, both segments and the back plate) can be biased separately. Due to the diaphragm, which protrudes from the tunnel by 0.5 mm around the entire circumference, the electrons should in principle not be able to reach the tunnel segments at any potential of all electrodes. XOOPIC simulations [7] of the original Katsumata configuration show that all electrodes should be swept at the same potential, to have parallel equidistant potential surfaces. We have followed this approach at first. However, it turned out that the back plate draws a strong electron current which disturbs the plasma in front of the tunnel. Therefore it has been left floating during our experiments.

Thus, for these measurements, the voltage was swept simultaneously in a range of about  $-100 < V_s < +100$  V across the diaphragm and the two tunnel segments. All sweeping voltages were kept equal in order to avoid arcing. The resulting three IV-characteristics are recorded separately. The IV-characteristic of the diaphragm, which faces the plasma, is conventional and contains both, the ion and electron current branches, from which the electron temperature  $T_e$  and the floating potential  $V_{fl}$  can be determined. Also the plasma potential  $\Phi_{pl}$  was determined from the inflection point of the characteristic after taking the logarithm. To get an idea about the ion density, in addition the ion saturation current to the diaphragm,  $I_{i, dia}$  was determined at 100 V below the plasma potential  $\Phi_{pl}$ . The IV characteristic of the first segment, which indeed is almost free of electron current, can be used to determine the perpendicular ion temperature  $T_{i, \perp}$  from the exponential drop of the ion current with increasing segment voltage.

In addition, we have determined the ion saturation currents to the two tunnel segments  $I_{i, 1, 2}$  at 100 V below the plasma potential  $\Phi_{pl}$ . The total ion saturation current to the tunnel,  $I_t = I_{i, 1} + I_{i, 2}$ , was compared to the ion saturation current to the diaphragm,  $I_{i, dia}$ . The ratio  $I_{i, 2} / I_{i, 1}$  of the two currents has been taken as an indication for  $T_{i, \parallel}$ . However, the precise relation between this ratio and  $T_{i, \parallel}$  has still to be determined by means of a XOOPIC simulation of this probe.

### 3 Results and Discussion

Fig. 2 a) and b) shows typical current-voltage characteristics of the left-hand side tunnel (with diaphragm). The IV characteristics of Fig. 2 have been registered at a radial position of  $r_p = 79$  mm, the Katsumata tunnel is oriented upstream to the toroidal plasma current. During a part of the flat top phase of the discharge, an additional electrode, inserted radially at  $r_E = 60$  mm near the position of the last-closed flux surface (LCFS) was biased to a voltage of +100 V. A more detailed description of the biasing experiment on CASTOR can be found in [8]. Fig. 2 a) shows the IV characteristics during the ohmic part, Fig. 2 b) shows those during biasing. The upper characteristics are those of the diaphragm, from which the indicated  $T_e$  values ( $T_e \cong 9.9$  eV for the ohmic and  $T_e \cong 12.5$  eV for the biasing phase of the discharge) have been determined. These values appear to be comparable to other probe measurements in the scrape-off layer (SOL) of CASTOR.

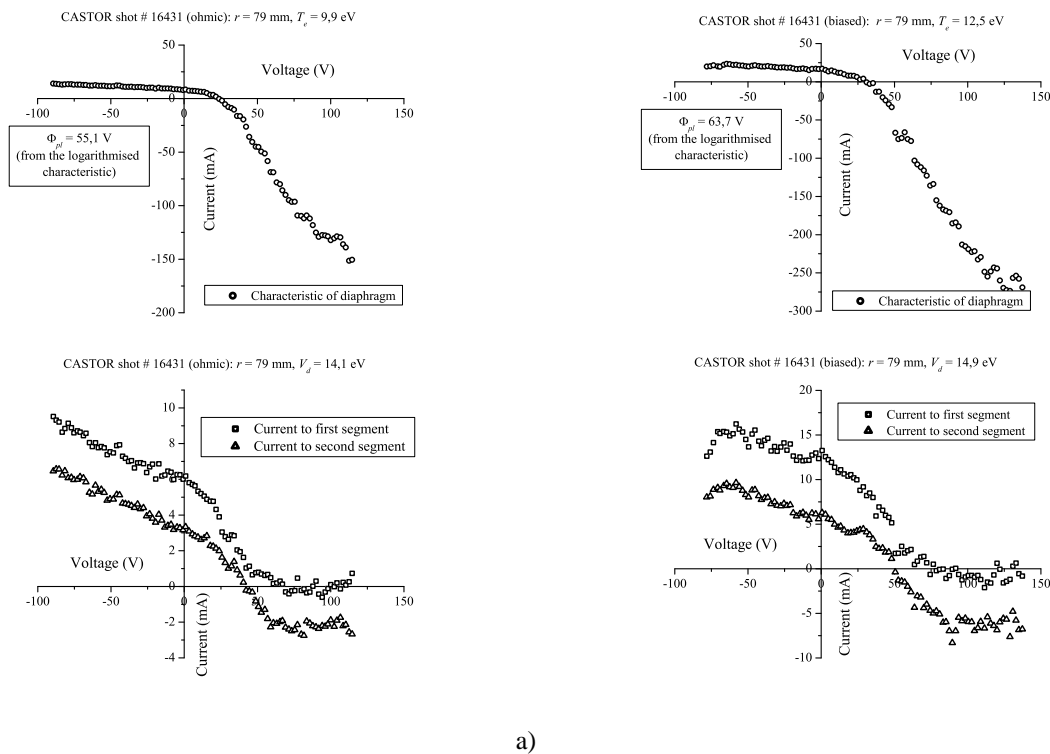


**Fig. 2** Typical current-voltage characteristics registered by the left-hand side tunnel (with diaphragm) during ohmic discharges a) and with edge biasing b). The upper curves (circles) show the characteristics of the diaphragm. The lower curves show the characteristics of the first tunnel segment (squares) and of the second tunnel segment (triangles).

We notice that with biasing,  $T_e$  is somewhat higher than without. This is a general trend also for other radial positions (see Fig. 4). The lower plots are IV characteristics of the first and the second segment. All the characteristics are of a similar shape. When the sweeping voltage  $V_s$  increases from negative values, the ion current decays approximately linearly. For  $V_s$  higher than the floating potential (see the IV characteristics of the diaphragm) the ion currents start to decay exponentially approximately like  $I_{i,1} \approx \exp(-V_s/V_d)$ . The characteristic constant of the exponential decay  $V_d$  should be proportional to the perpendicular ion temperature  $T_{i,\perp}$ . Generally the values for ohmic and biased discharges are almost equal for all measured radial positions.

It is seen that the electron screening by the diaphragm works properly only for the first segment, where the current decays to almost zero as it was expected. Unfortunately, however, a non-negligible electron current is seen to reach the second segment. Consequently, the indicated values of  $V_d \cong 14.1$  eV for the ohmic and  $V_d \cong 14.9$  eV for the biased part of the discharge were determined only from the characteristics of the first segment. In

general these two values are very similar so that obviously the fact whether or not the electrode is biased has not much influence on the perpendicular ion temperature.

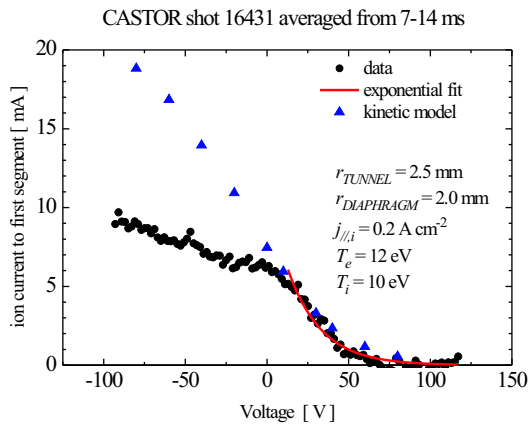


**Fig. 3** Real IV characteristic (solid circles) of the first segment (same as Fig. 2 a) above) and simulated characteristic (triangles) obtained from an XOOPIK code simulation with the parameters indicated. The solid line shows the exponential fit from which a value of  $V_d \approx 30$  eV was determined. The discrepancy of this value from the measured one still needs further investigation.

In order to interpret the IV characteristics to the first segment, we have performed preliminary kinetic simulations of the measured IV characteristic to the first segment. The XOOPIK code was run several times varying the tunnel and diaphragm voltage. The initial plasma parameters were chosen as  $T_i = 10$  eV,  $T_e = 12$  eV, and  $j_{\parallel,i} = 0.2$  A/cm<sup>2</sup>, where this latter quantity is the parallel ion current density into the tunnel, determined from the ion saturation current of the diaphragm. The specified initial value of  $T_i$ , used for the simulation, namely 10 eV, is the temperature for the total energy distribution, without specification of the velocity component parallel or perpendicular to **B**. Fig. 3 shows a comparison of the simulation results (triangle) with the measured characteristic (solid circles) of the first segment for the ohmic part of the discharge (from Fig. 2 a). The code reproduces the ion current for positive retarding voltages quite well. However, the characteristic constant of the exponential decay  $V_d$  from experiment as well as from simulations is roughly three times higher than the perpendicular ion temperature, for which the simulation is performed. Understanding this discrepancy will be subject of future investigations.

Fig. 4 shows radial profiles of all measured quantities in a range of  $57 < r < 92$  mm, with the position of the biased electrode at  $r_E = 60$  mm. The radial position of the LCFS is 73 mm. The solid squares show always the values for the ohmic part of the discharges, whereas the solid circles show the values taken during the biased part of the discharge.

The results can be summarised as follows:

- Figs. 4 a) and b) show the radial profiles of the ion saturation currents to the diaphragm ( $I_{i, dia}$ , Fig. 4 a) and to the entire tunnel ( $I_t = I_{i,1} + I_{i,2}$ , Fig. 4 b)). All four currents drop with  $r$ ; in both cases the values are generally higher for the biased part of the discharges than for the ohmic parts.
- The radial profile of the electron temperature, shown in Fig. 4 c), shows a drop of  $T_e(r)$  with  $r$ . In general, the values for the biased parts of the discharges are somewhat higher outside the LCFS (separatrix at  $r \cong 73$  mm), whereas the opposite is the case inside.
- The radial plasma potential profiles are shown in Fig. 4 d). For the ohmic discharges we observe a maximum of about 60 V at  $r \cong 75$  mm, which corresponds to the position of the LCFS. The radial profile is, however, strongly modified by the biasing of the electrode located at  $r_E = 60$  mm. In this range of radii we see a clear maximum of  $\Phi_{pl}$  at more than +100 V, which is comparable to the biasing voltage.
- The radial profiles of the parameter  $V_d$ , (Fig. 4 e)) show an increase of the values with  $r$ , which may suggest that in the SOL the ion temperature is higher than inside the separatrix. This result is somewhat surprising and needs further detailed investigations. For both, the ohmic and for the biased parts of the discharges, the resulting values of  $T_{i,\perp}$  seem to be similar.

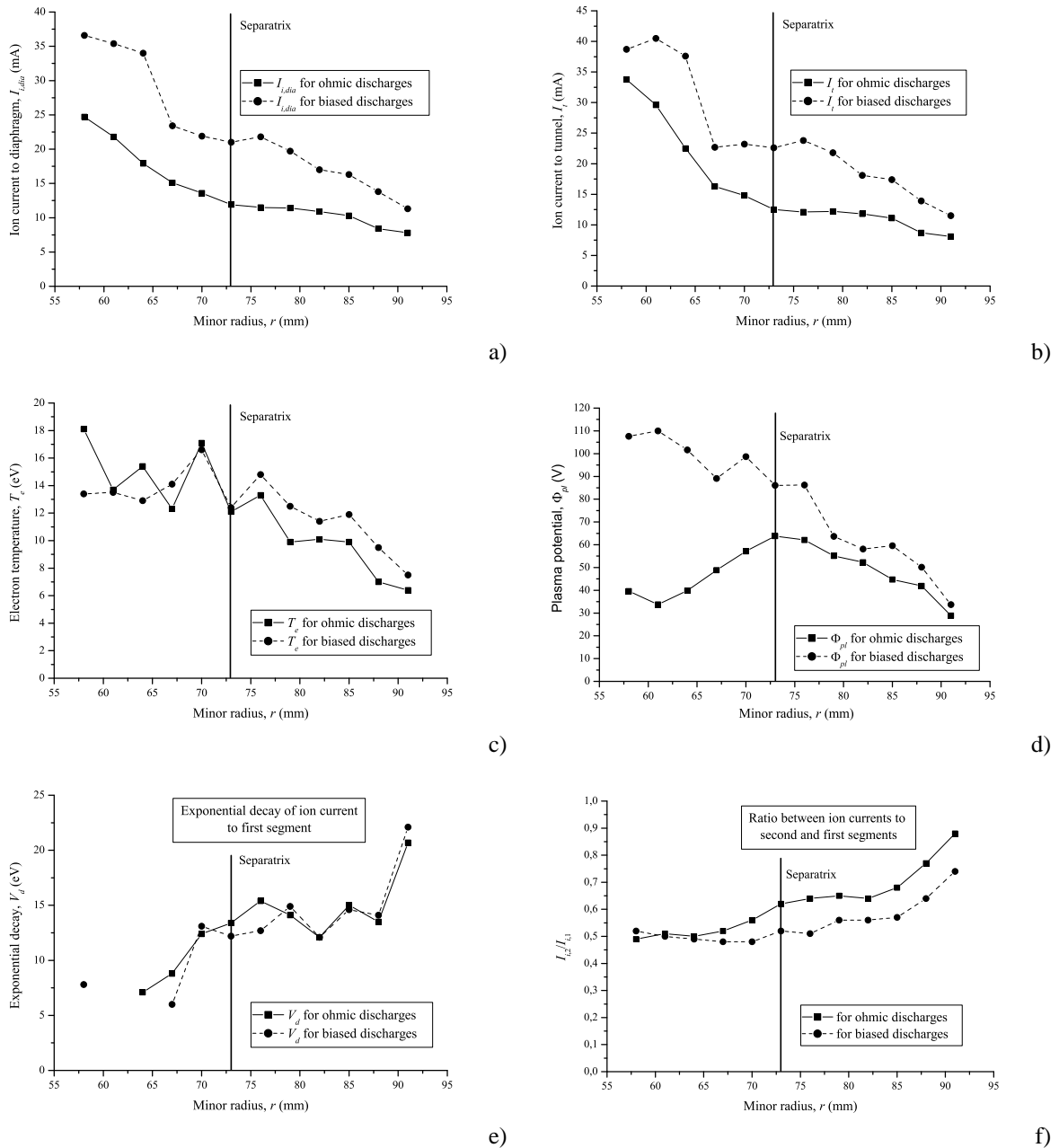


**Fig. 4** Radial profiles of the ion saturation currents to the diaphragm a), the tunnel b), the electron temperature  $T_e$  c), the plasma potential  $\Phi_{pl}$  d), the slope of the exponential decay  $V_d$ , which gives a measure for the perpendicular ion temperature  $T_{i,\perp}$  e), and of the ratio  $I_{i,2}/I_{i,1}$  between the ion saturation currents to the two segments, which gives a measure for the parallel ion temperature  $T_{i,\parallel}$  f). In all four cases the solid squares show the values for the ohmic parts of the discharges, while the solid circles show the values for the biased parts.

- Also the ratio  $I_{i,2}/I_{i,1}$  (Fig. 4 f)) of the saturation currents to the two segments, which can be considered as a measure for  $T_{i,\parallel}$ , increases towards the edge, however, in this case the biased parts of the discharges always deliver lower values. Since the ion saturation currents increase for lower values of the voltage  $V_s$ , the saturation currents have always been taken at a value of -100 V below the respective values of the plasma

potential. The ratio  $I_{i,2}/I_{i,1}$  has been chosen such since we wanted to obtain values which would increase with the parallel ion temperature. Clearly, these values are subject to great random and systematic errors.

It is clear that the radial profiles of  $V_d$  and  $I_{i,2}/I_{i,1}$  (Figs. 4 e) and f)), shown above, need not necessarily correspond to those of the perpendicular and parallel ion temperatures. We emphasise again that the PIC simulations have been performed only for a single set of input parameters (see Fig. 3) and we can not exclude any variation of  $V_d$  and  $I_{i,2}/I_{i,1}$  with the parallel ion flux into the tunnel and also with the electron temperature. Both these quantities change significantly with the radius as evident from Figs. 4 a) and b).

## 4 Conclusion

In conclusion, the preliminary measurements with the segmented Katsumata tunnel probe look promising. The PIC simulations are able to describe some features of the probe performance. However, more effort is definitely required to reach concordance between the simulations and measurements for the whole range of applied voltages. It is clear that the observed collection of electrons by the second tunnel can not be simulated by PIC code, unless collisions or other phenomena are taken into account. It is evident that the Katsumata tunnel can be routinely used for measurements of the edge ion temperature only after solving all above mentioned problems.

**Acknowledgements** This work has been carried out within the Association EURATOM-ÖAW, within the Association EURATOM/ENEA and within the Association EURATOM-IPP.CR under contract. The content of the publication is the sole responsibility of its author(s) and it does not necessarily represent the views of the Commission or its services. Part of the work was performed in frame of the project 202/03/0786 (Grant Agency of the Czech Republic) and 2001-2056 (INTAS). The work was partly supported by the FWF (Austria) under grant No. P14545-PHY.

## References

- [1] I. Katsumata, M. Ozazaki, Japan. J. Appl. Phys. **6**, 123 (1967).
- [2] I. Katsumata, Contrib. Plasma Phys. **36**, 73 (1996).
- [3] J.P. Gunn, Phys. Plasmas **8**, 1040 (2001).
- [4] J.P. Gunn et al., Czech J. Phys. **52**, 1107 (2002).
- [5] J. Verboncoeur et al., Comput Phys. Commun. **87**, 199 (1995).
- [6] K. Uehara, A. Tsushima, H. Amemiya and JFT-2M Group, J. Phys. Soc. Japan **66**, 921 (1997).
- [7] N. Ezumi, Contrib. Plasma Phys. **41**, 488 (2001).
- [8] G. Van Oost et al., Plasma Phys. Control. Fusion **45**, 621 (2003).